Supplementary materials

Core-satellite micellar system against primary tumor and its lymphatic metastasis through modulation of fatty acid metabolism blockade and tumor-associated macrophages

Xuan He [a], Tao Deng [a], Jiaxin Li [a], Rong Guo [a], Yashi Wang [a], Ting Li [a], Shuya Zang [a], Jiaxin Li [a], Ling Zhang [b], Man Li [a]*, Qin He [a]*

[a] Key Laboratory of Drug-Targeting and Drug Delivery System of the Education Ministry and Sichuan Province, Sichuan Engineering Laboratory for Plant-Sourced Drug and Sichuan Research Center for Drug Precision Industrial Technology, West China School of Pharmacy, Med-X Center for Materials, Sichuan University, China.

[b] College of Polymer Science and Engineering, Sichuan University, China.

*Corresponding author: Tel: +86-28-85502532 Fax: +86-28-85502532

E-mail: manli@scu.edu.cn; qinhe@scu.edu.cn

Materials and methods

Determination of Critical micellar concentration (CMC)

The critical micelle concentration (CMC) of obtained amphiphilic polymers of PCL-PEG-Me, PCL-PEG-COOH and PCL-PEG-Pep were determined by pyrene fluorescent probe method. In detail, pyrene was dissolved in acetone to obtain 1.5×10^{-5} mol/L pyrene solution. Then 80 μL pyrene stock solution was added to 2 mL brown volumetric flasks and the acetone was removed in dark and ventilated condition. Next, a series of PCL-PEG-Me, PCL-PEG-COOH and PCL-PEG-Pep micelles with concentration of 0.25 ~ 500 μg/mL were added to 2 mL brown volumetric flasks, then incubating in the dark for 24 h (37 ℃, 75 rpm). Fluorescence spectrophotometer (RF-6000, Shimadzu, Japan) was used to measure the fluorescence intensity of soluble pyrene with Ex = 372 nm and Em = 382 nm. CMC was calculated by plotting the curve of the intensity ratio (I_{372}/I_{382}) to LogC (C corresponds to micelle concentration).

Hemocompatibility and serum stability

To evaluate the hemolytic effect of micelles, the whole blood of mice was collected into heparinized tubes and centrifuged to collect the erythrocytes. PCL@DSPE and PCL-DSPE were suspended in 2% erythrocytes suspensions with final concentration of 1 mg/mL, 2 mg/mL, and 4 mg/mL, respectively. 1% Triton-X-100 served as the positive group and PBS (pH 7.4) was the negative group. During incubation, the mixture was centrifuged at a series of predetermined timepoints and photographed. Finally, the absorption of each supernatant at 540 nm was determined by Varioskan Flash Multimode Reader (Thermo Fisher, USA).

For serum stability of micellar systems, PCL-DSPE, PCL@DSPE, PCL/PTX-DSPE/ET and PCL/PTX@DSPE/ET were prepared and then mixed with FBS (formulation: FBS (v/v) of 9:1, 1:1; micelle concentration was 1 mg/mL). The mixture was incubated under 37 °C, 90 rpm, respectively. At the predetermined timepoint (0, 1, 2, 4, 8, 12 and 24 h), the absorption of samples at 750 nm were

measured by Varioskan Flash Multimode Reader and the transmittance were calculated.

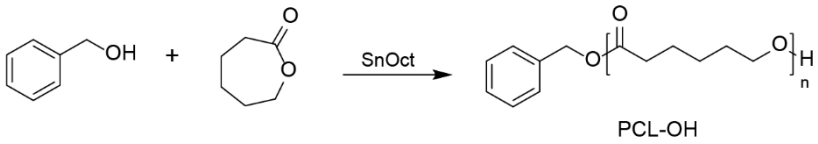

Scheme S1. The synthesis route of PCL-OH.

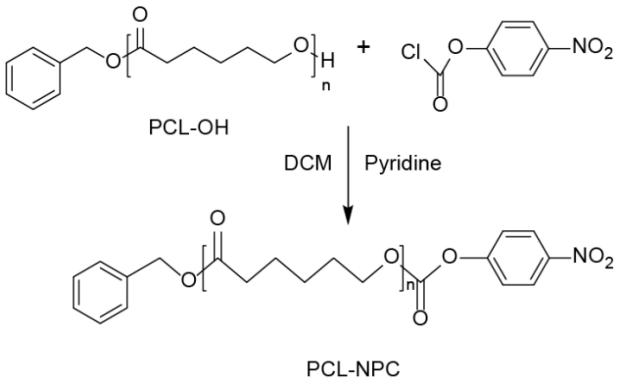

Scheme S2. The synthesis route of PCL-NPC.

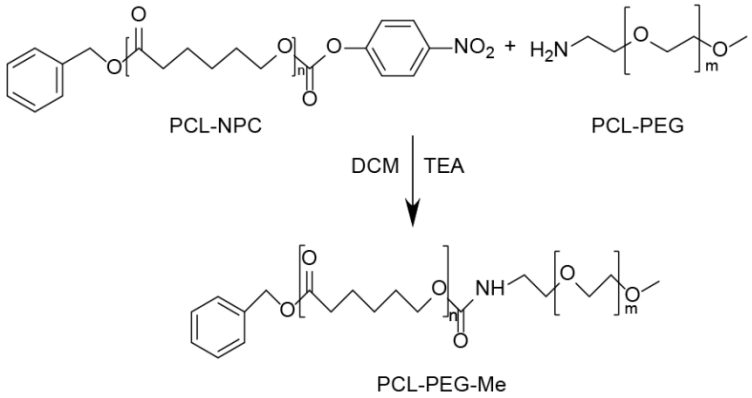

Scheme S3. The synthesis route of PCL-PEG-Me.

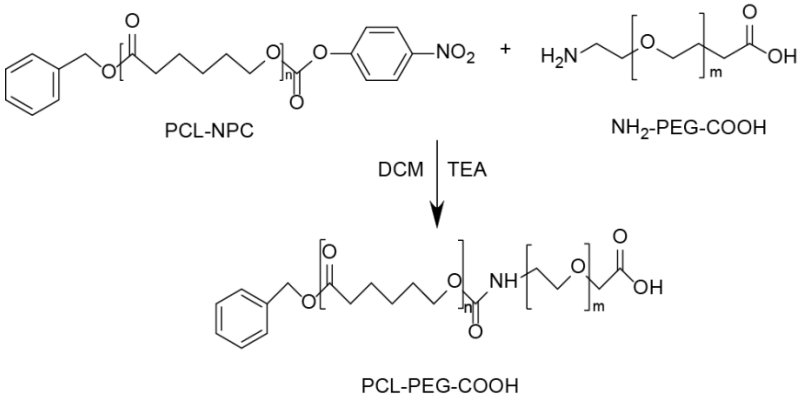

Scheme S4. The synthesis route of PCL-PEG-COOH.

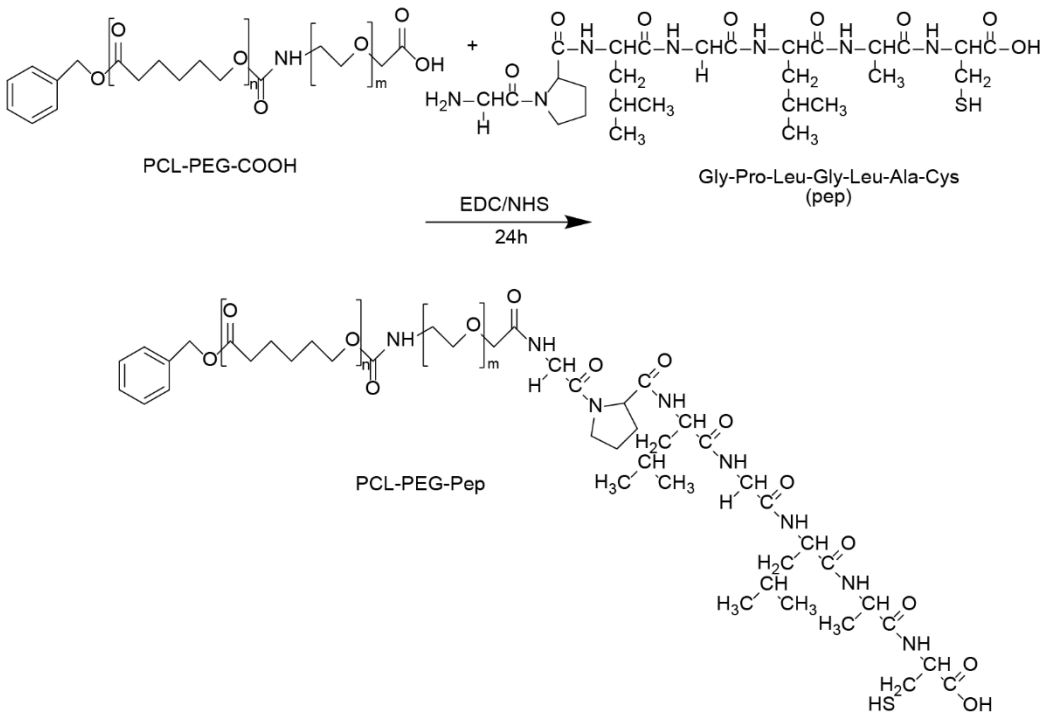

Scheme S5. The synthesis route of PCL-PEG-Pep.

Table S1. Molecular weight of PCL-OH, PCL-PEG-Me and PCL-PEG-Pep determined by GPC.

Polymer	Mn (Dalton)	Mw (Dalton)	Mw/ Mn
PCL-OH	6,558	8,694	1.326
PCL-PEG-COOH	9,893	13,570	1.372
PCL-PEG-Pep	10,488	14,435	1.376

Table S2. Encapsulation efficiency and drug loading of PTX and Etomoxir. [n = 3, mean ± SD]

Groups	PTX-EE (%)	PTX-DL (%)	ET-EE (%)	ET-DL (%)
PCL/PTX@DSPE/ET	96.87±1.14	4.50±0.17	83.55±1.10	1.37±0.24
PCL/PTX-DSPE/ET	95.68±1.34	4.39±0.56	83.31±0.80	1.25±0.36

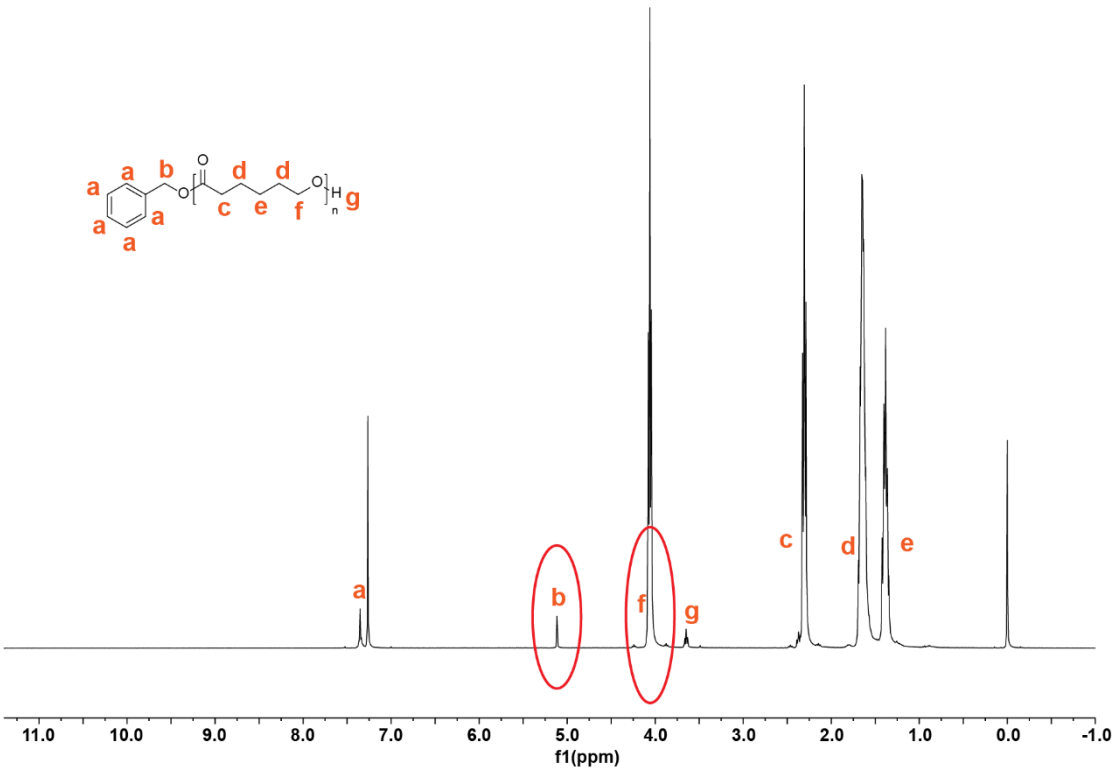

Figure S1. The ^{1}H-NMR spectrum of PCL-OH. The sample was dissolved in chloroform-D ($CDCl_3$) for the measurements.

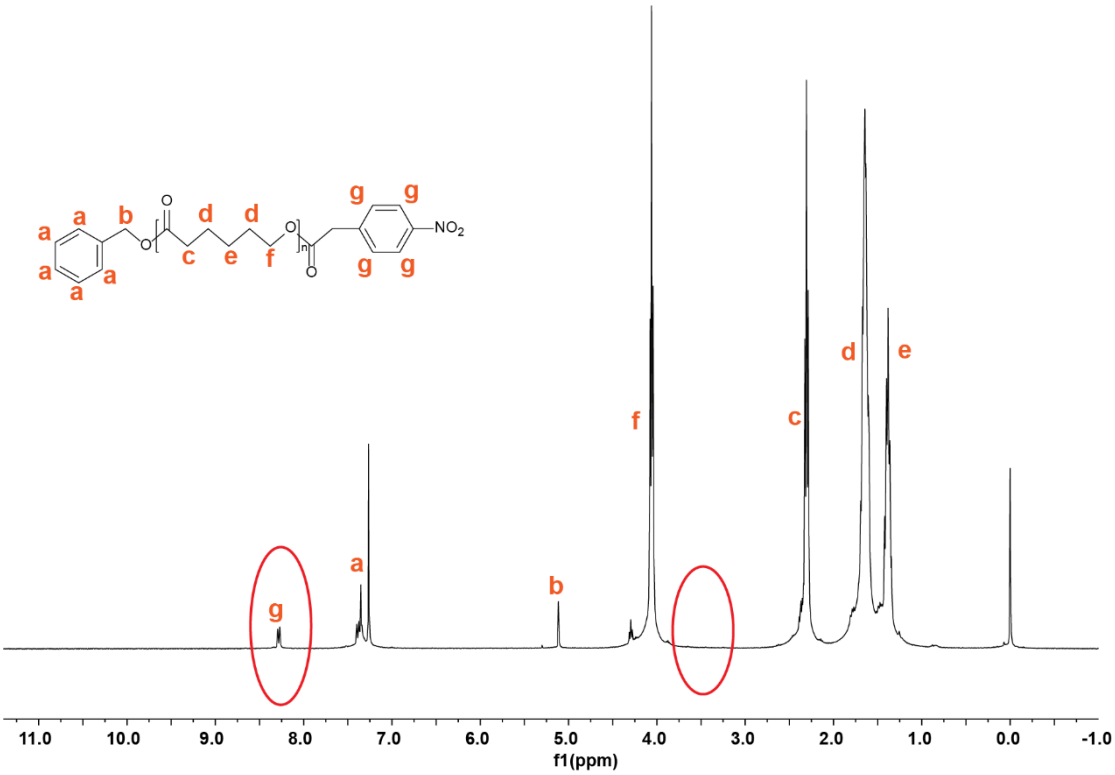

Figure S2. The ^{1}H-NMR spectrum of PCL-NPC. The sample was dissolved in chloroform-D ($CDCl_3$) for the measurements.

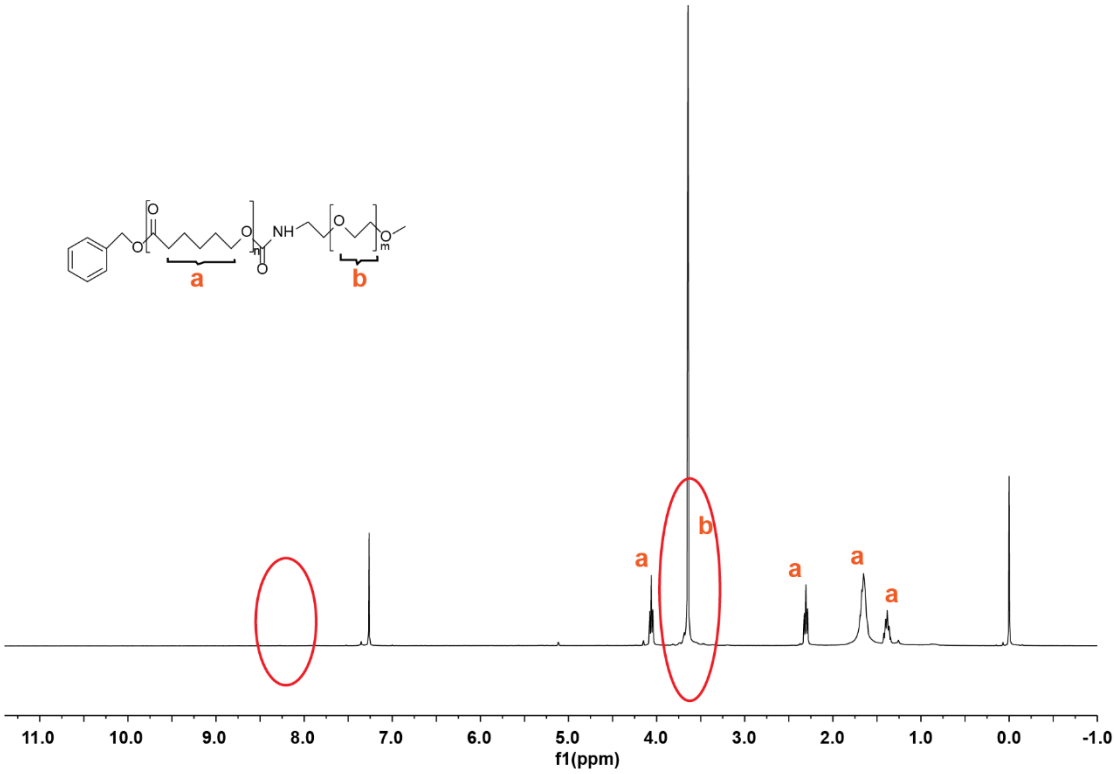

Figure S3. The ^{1}H-NMR spectrum of PCL-PEG-Me. The sample was dissolved in chloroform-D ($CDCl_3$) for the measurements.

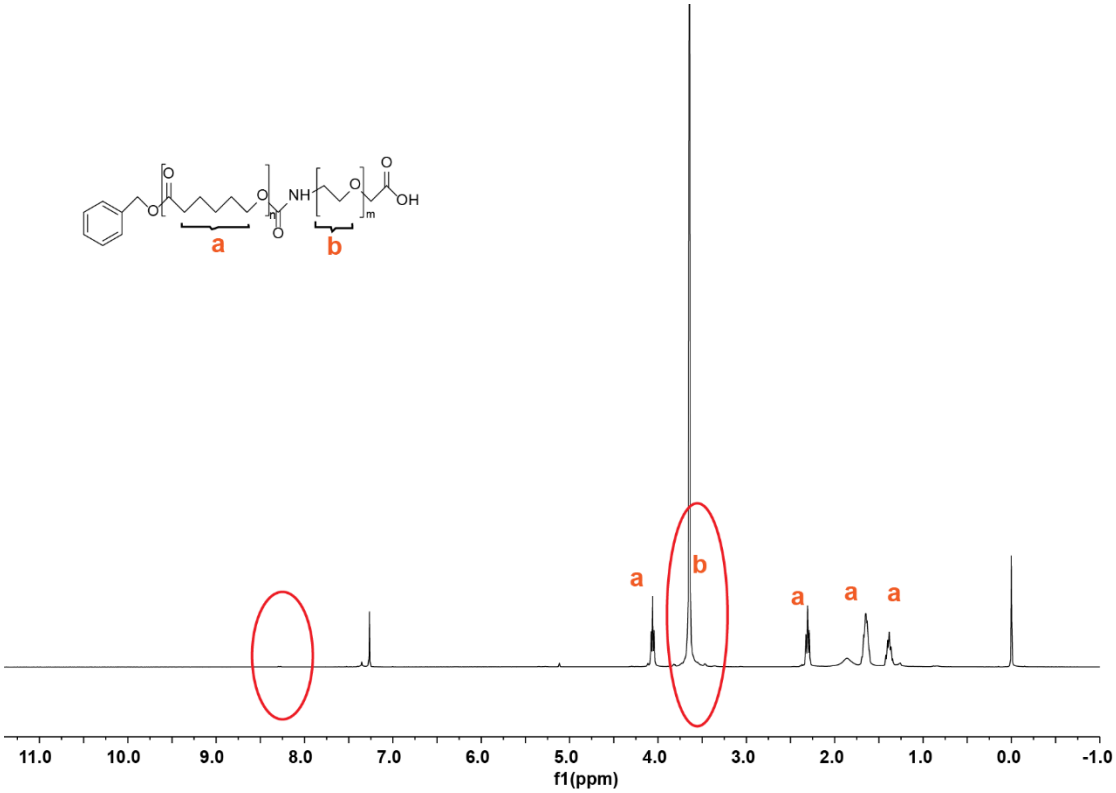

Figure S4. The ^{1}H-NMR spectrum of PCL-PEG-COOH. The sample was dissolved in chloroform-D ($CDCl_3$) for the measurements.

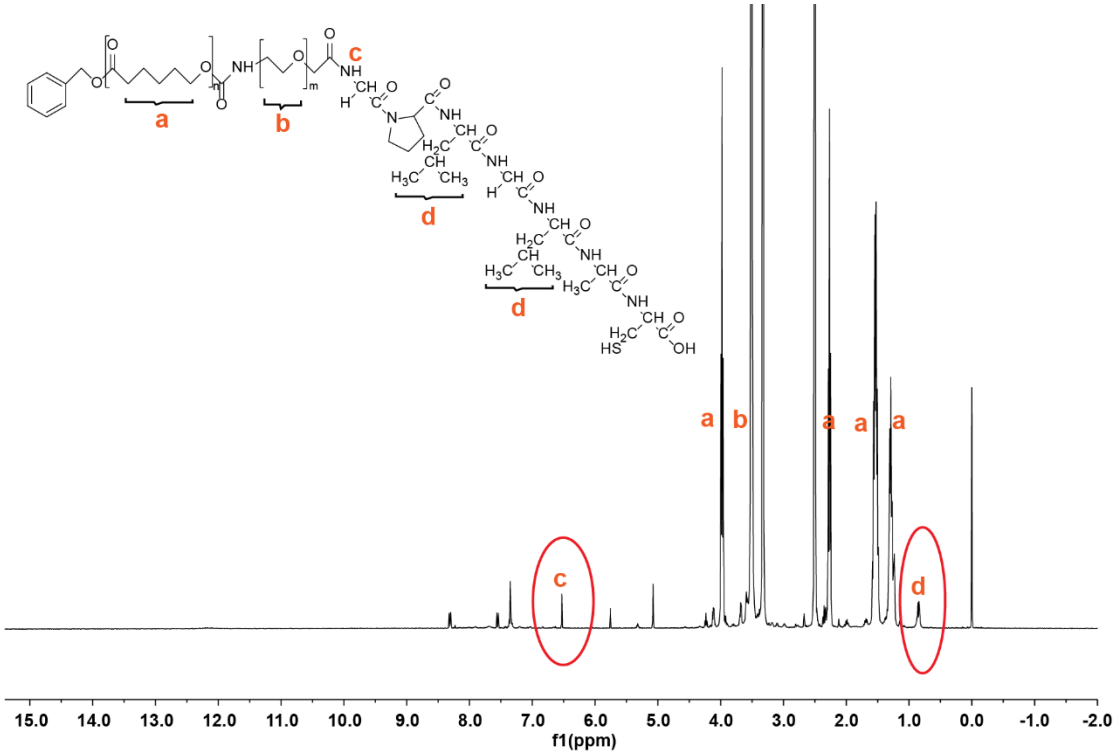

Figure S5. The ^{1}H-NMR spectrum of PCL-PEG-Pep. The sample was dissolved in DMSO for the measurements.

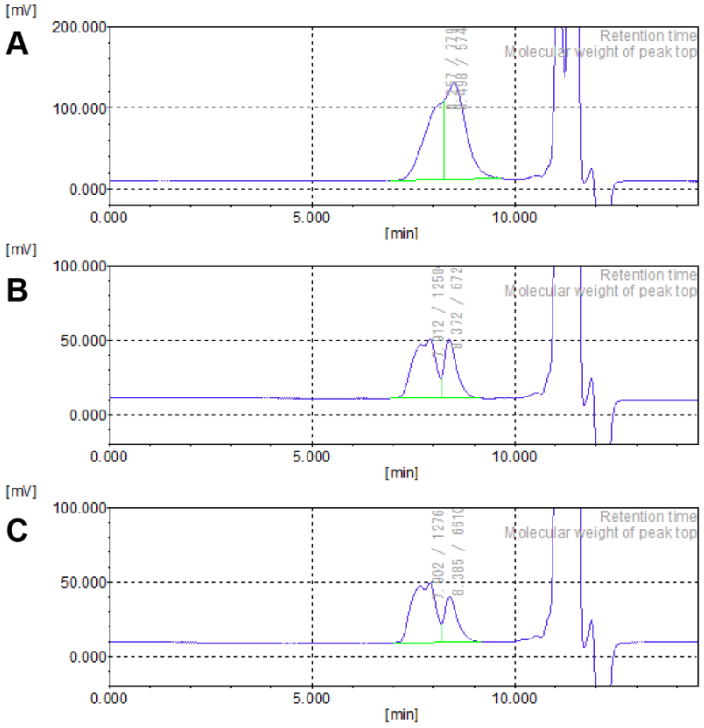

Figure S6. Chromatographic traces curves of (A) PCL-OH, (B) PCL-PEG-COOH and (C) PCL-PEG-Pep over time by GPC.

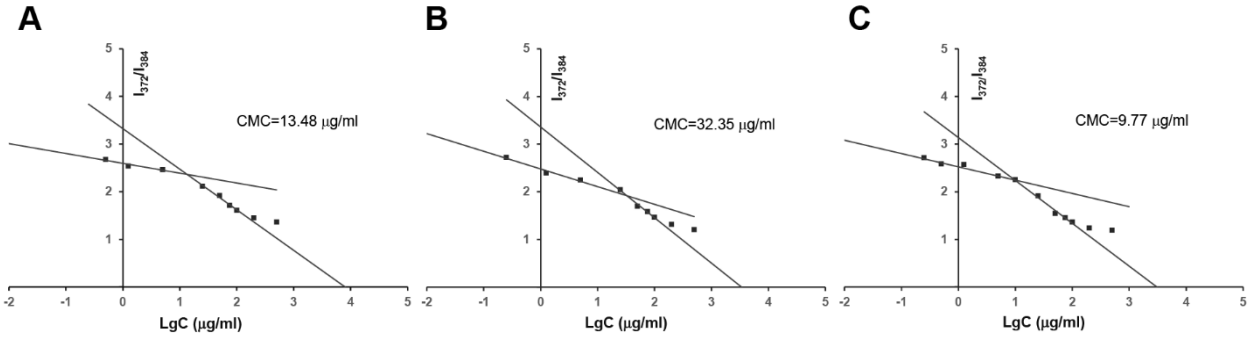

Figure S7. Critical micelle concentration (CMC) of (A) PCL-PEG-Me, (B) PCL-PEG-Pep, (C) PCL-PEG-COOH.

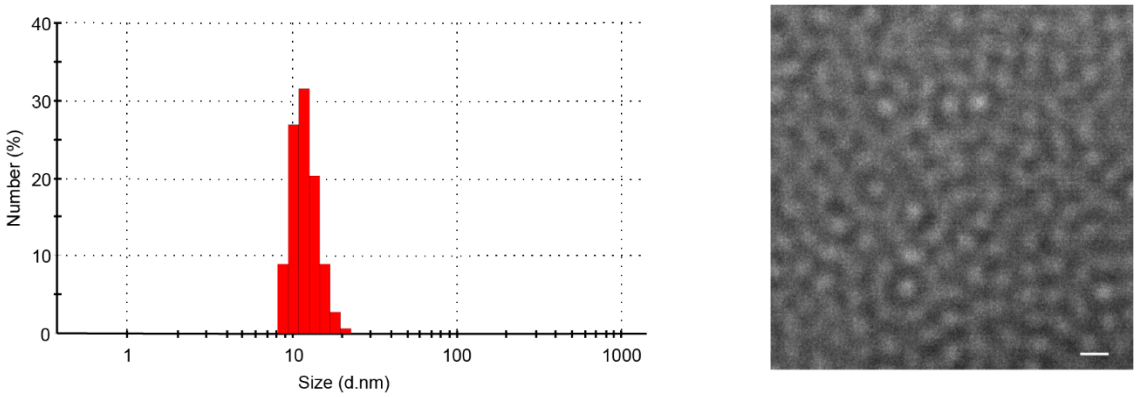

Figure S8. The size distribution and typical TEM images of DSPE-PEG/ET micelles. Scale bar: 10 nm.

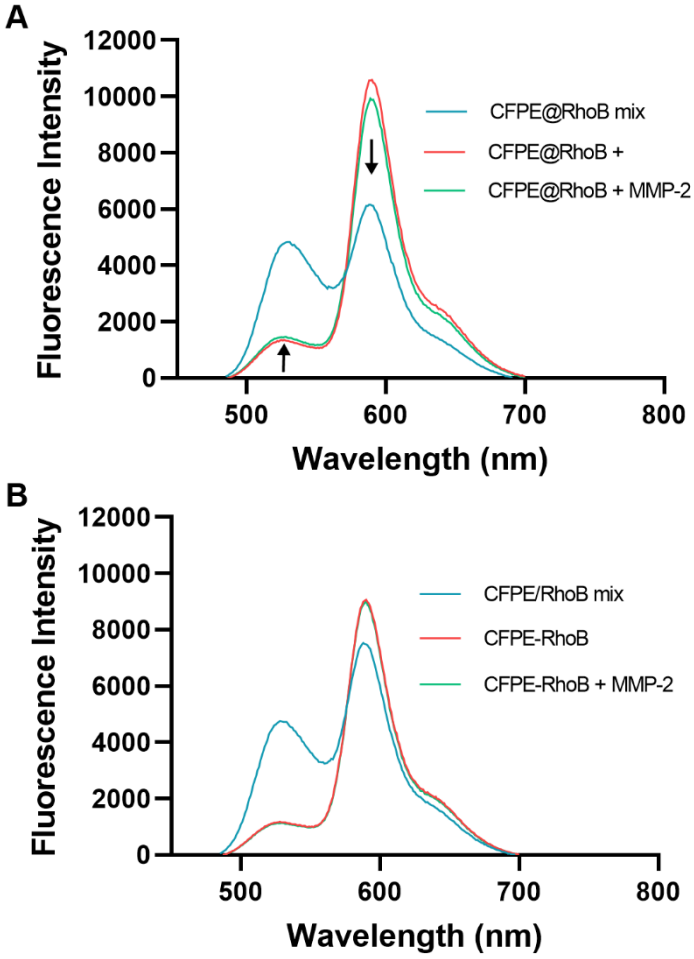

Figure S9. The of fluorescence emission spectra of (A) PCL/CFPE@DSPE/RhoB and (B) PCL/CFPE-DSPE/RhoB after incubating with MMP-2.

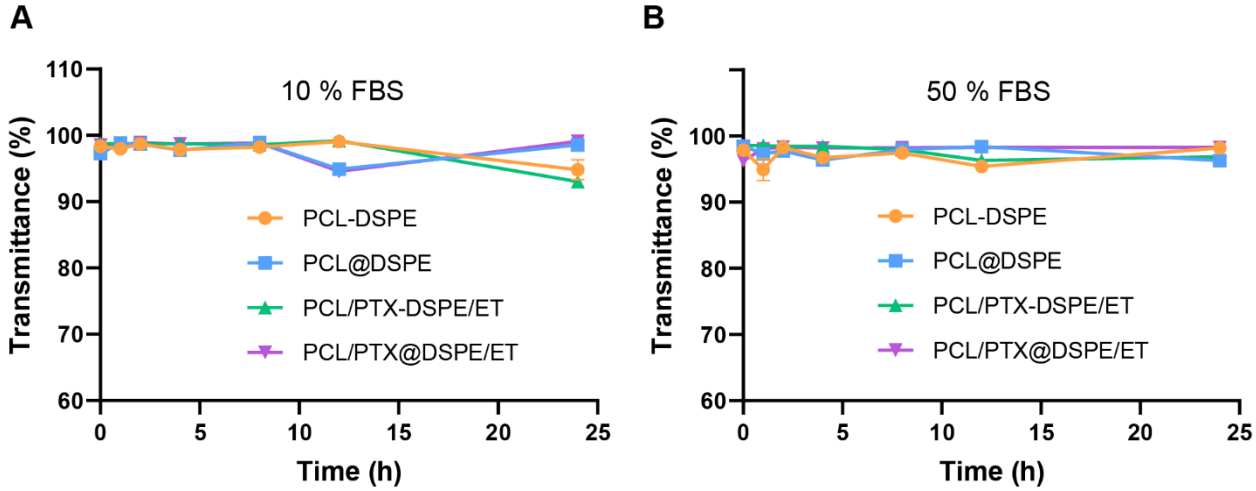

Figure S10. The stability of PCL-DSPE, PCL@DSPE, PCL/PTX-DSPE and PCL/PTX@DSPE/ET in (A) 10% FBS and (B) 50% FBS. [n = 3, mean ± SD]

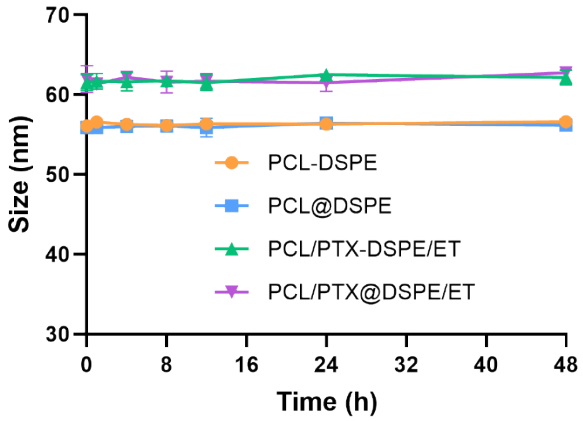

Figure S11. The hydrodynamic diameter curves of different formulations stored at 4 °C. [n = 3, mean ± SD]

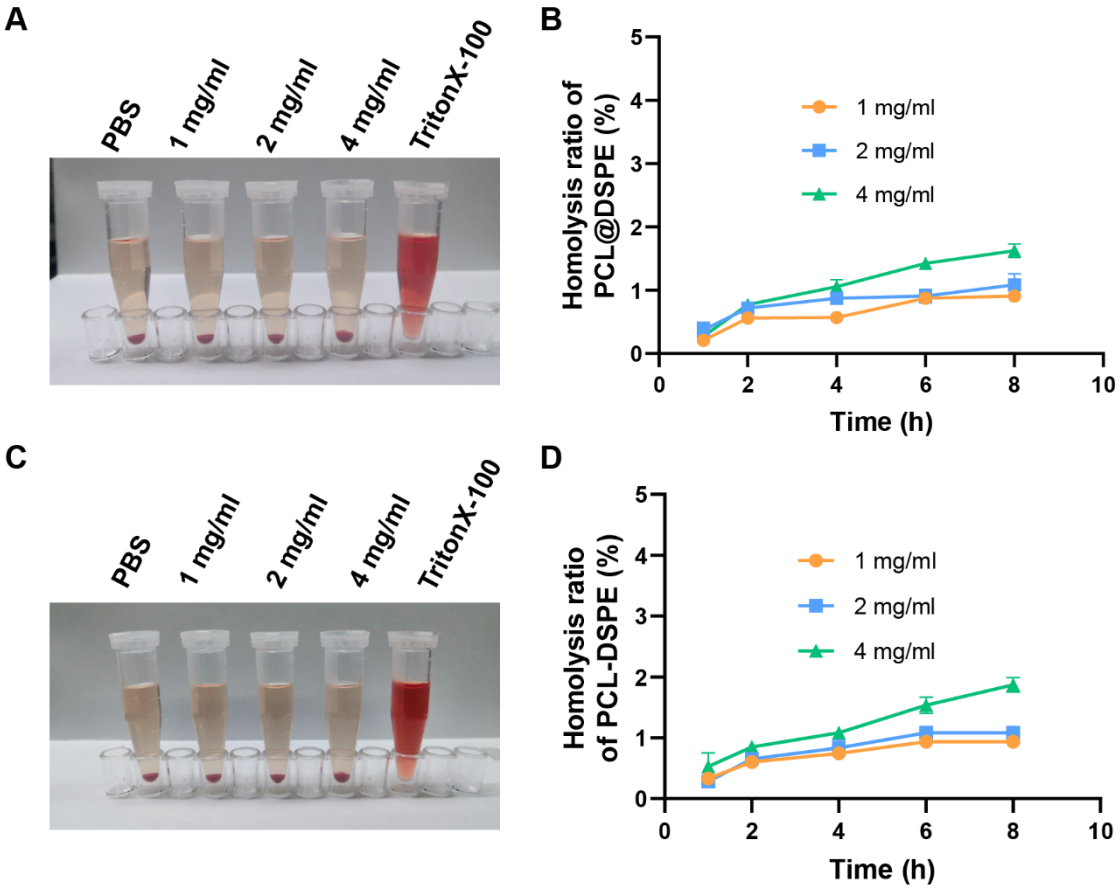

Figure S12. The hemolysis evaluation of (A, B) PCL@DSPE and (C, D) PCL-DSPE. [n = 3, mean ± SD]

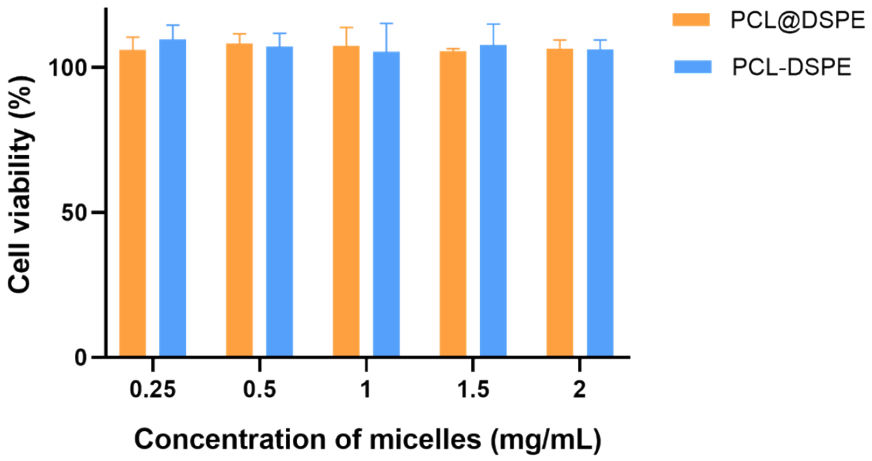

Figure S13. The 24 h cytotoxicity of blank micelles on 4T1 cells at different concentration. [n = 3, mean ± SD]

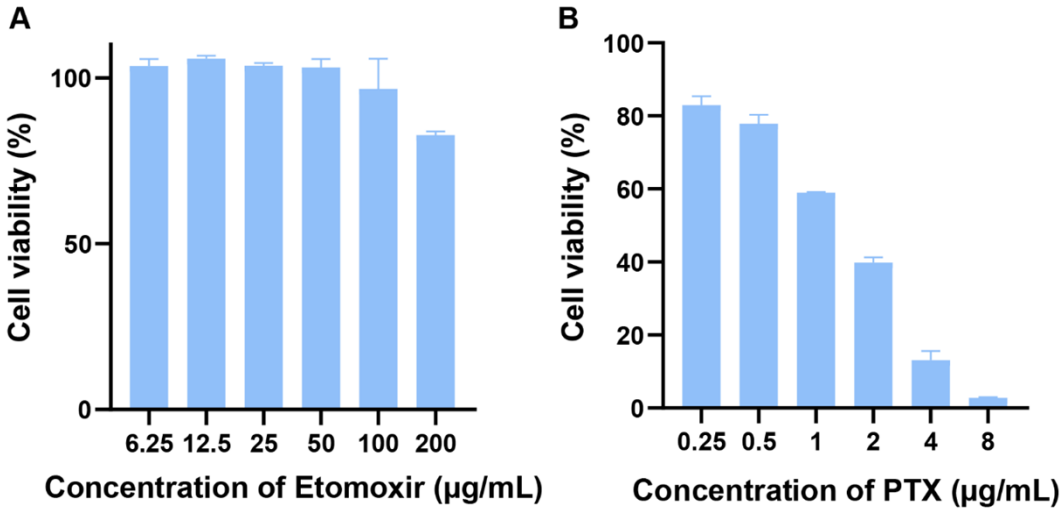

Figure S14. The cytotoxicity of (A) free Etomoxir and (B) PTX at different concentration on 4T1 cells after treatment for 24 h. [n = 3, mean ± SD]

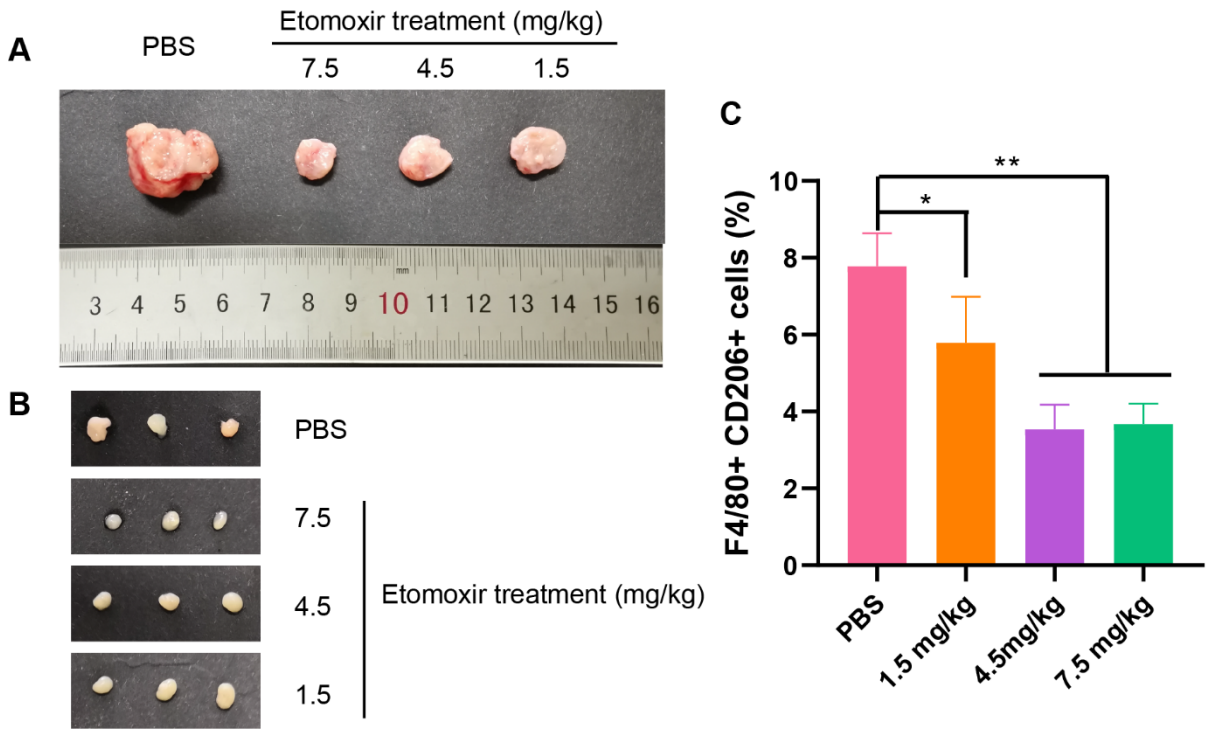

Figure S15. *In vivo* dosage determination of Etomoxir. Images of (A) tumor and (B) tumor-draining lymph nodes after treatment. (C) Tumor infiltration of $F4/80^{+}/CD206^{+}$ M2 macrophages. [n = 3, PTX= 3 mg/kg, Etomoxir at different dosage of 1.5 mg/kg, 4.5 mg/kg, and 7.5 mg/kg. * $p < 0.05$, ** $p < 0.01$.]

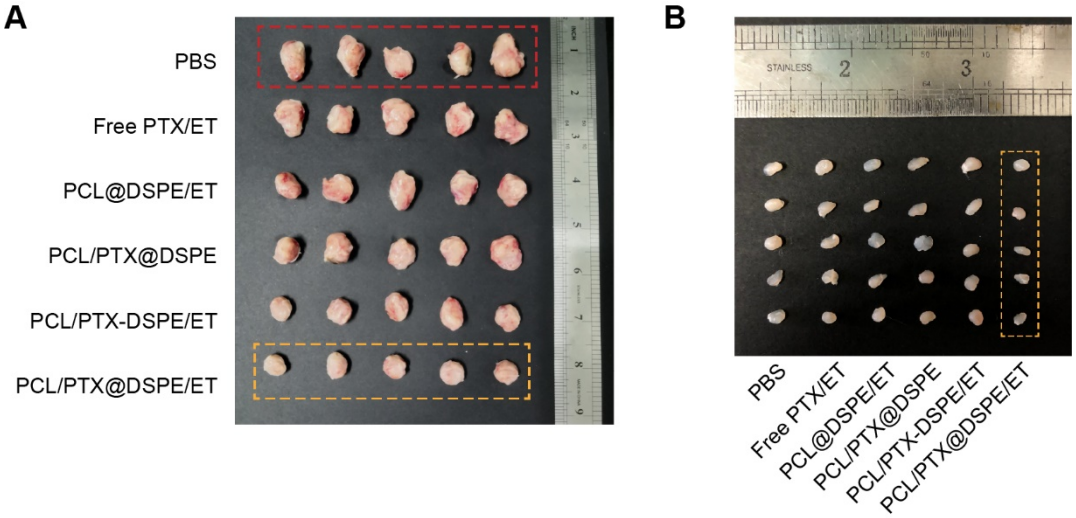

Figure S16. Representative photographs of (A) primary tumors and (B) tumor-draining lymph nodes isolated from 4T1 tumor-bearing mice on day 30. [n = 5]

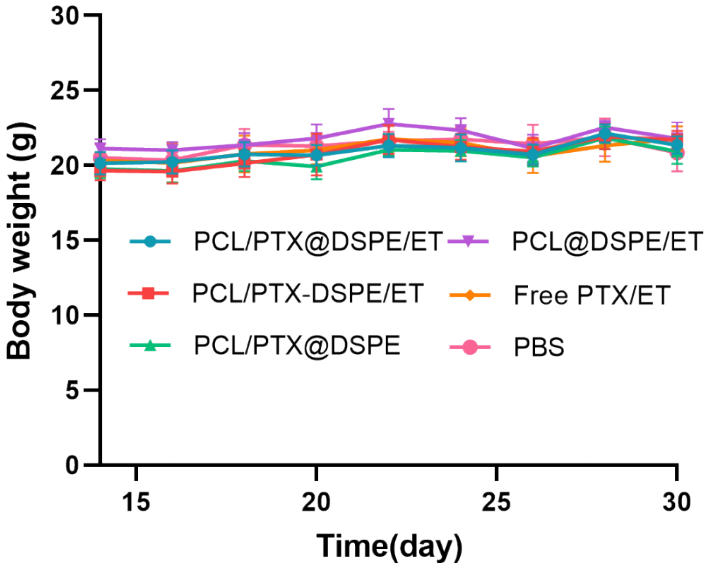

Figure S17. Body weight changes of Balb/c mice during treatment. [n = 5, mean ± SD]

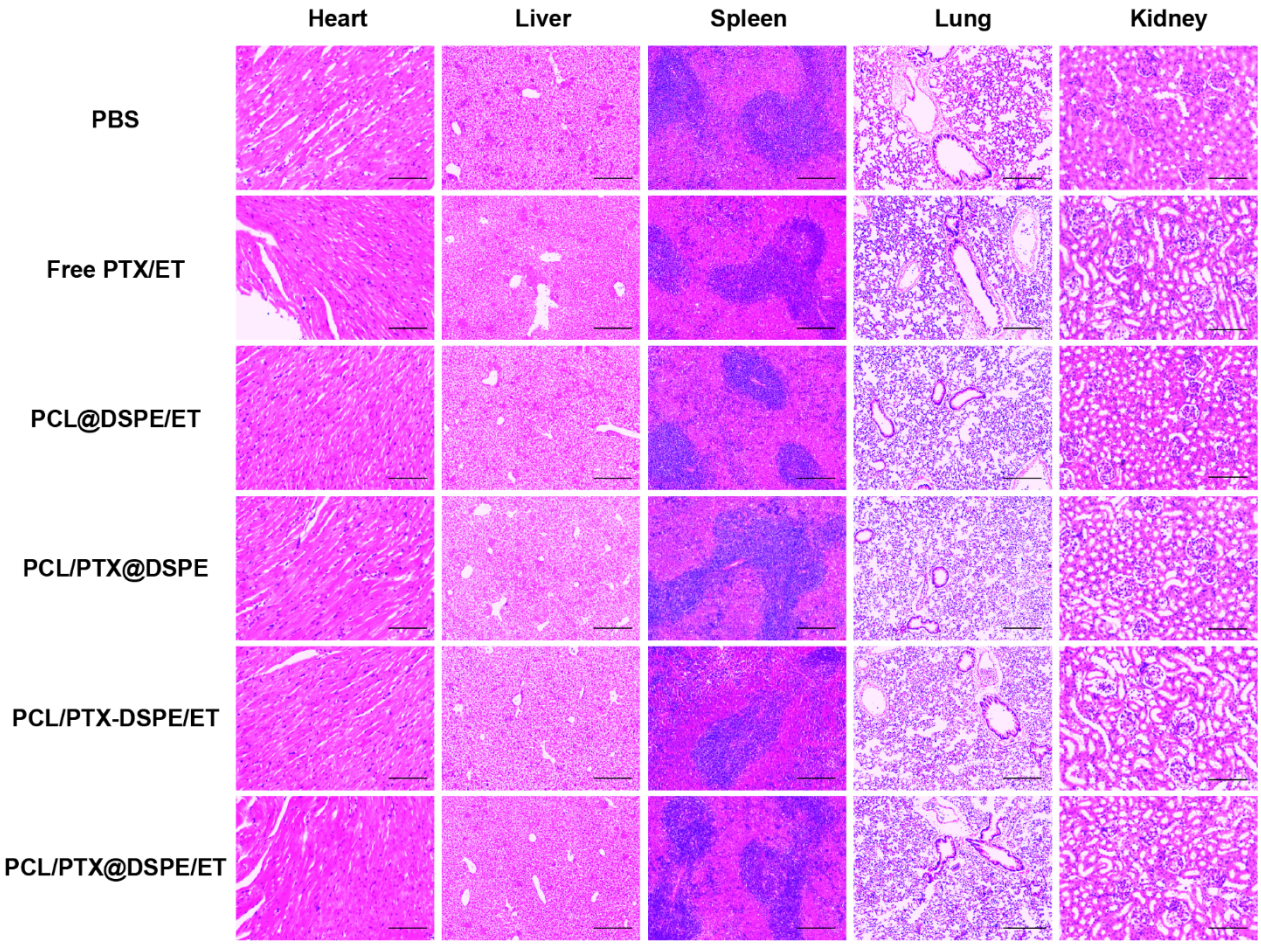

Figure S18. H&E staining pictures of heart, liver, spleen, lung, and kidney. Scale bar: 100 μm (heart and kidney), 250 μm (liver, spleen, and lung).

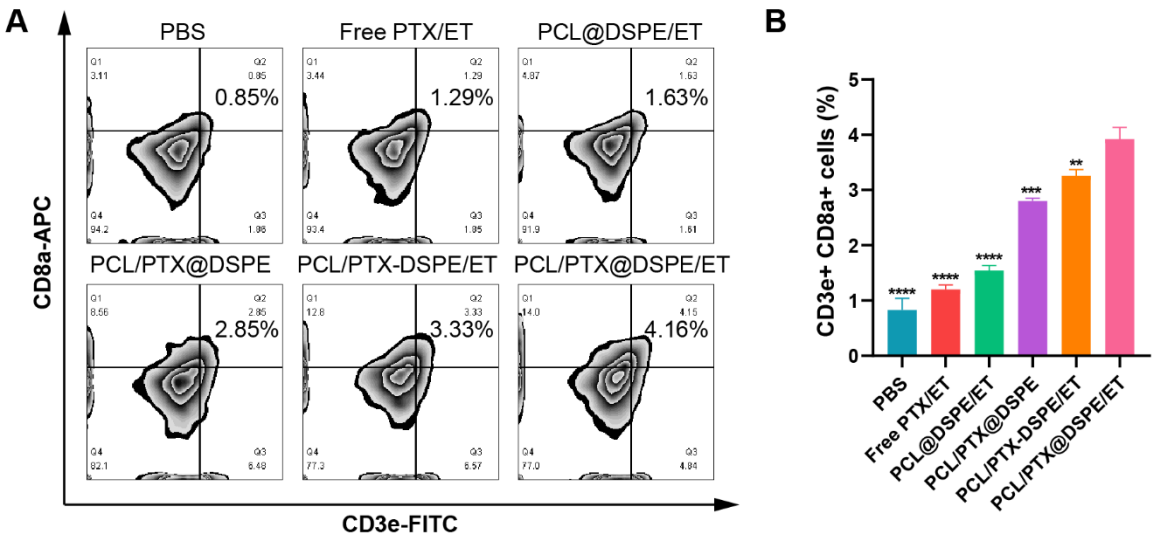

Figure S19. Relative population of $CD8^+$ T cells in tumor-draining lymph nodes after treatment. [n = 3, mean ± SD. ** $p < 0.01$, *** $p < 0.005$, **** $p < 0.001$.]